Self-adaptive electronic contact between graphene and semiconductors

Haijian Zhong, Zhenghui Liu, Gengzhao Xu, Yingmin Fan, Jianfeng Wang et al.

Citation: Appl. Phys. Lett. **100**, 122108 (2012); doi: 10.1063/1.3696671
View online: http://dx.doi.org/10.1063/1.3696671
View Table of Contents: http://apl.aip.org/resource/1/APPLAB/v100/i12
Published by the American Institute of Physics.

Self-adaptive electronic contact between graphene and semiconductors

Haijian Zhong,[1,2,a)] Zhenghui Liu,[1,a)] Gengzhao Xu,[1] Yingmin Fan,[1] Jianfeng Wang,[1,3] Xuemin Zhang,[1] Liwei Liu,[1] Ke Xu,[1,3,b)] and Hui Yang[1,3,c)]
[1]*Suzhou Institute of Nano-tech and Nano-bionics, CAS, Suzhou 215125, People's Republic of China*
[2]*Graduate University of Chinese Academy of Sciences, Beijing 100049, People's Republic of China*
[3]*Suzhou Nanowin Science and Technology Co., Ltd., Suzhou 215123, People's Republic of China*

(Received 19 September 2011; accepted 5 March 2012; published online 22 March 2012)

Understanding the contact properties of graphene on semiconductors is crucial to improving the performance of graphene optoelectronic devices. Here, we show that when graphene is in contact with a semiconductor, the charge carrier transport into graphene leads to a self-adaptive shift of the Fermi level, which tends to lower the barrier heights of the graphene contact to both *n*- and *p*-type semiconductors. A theoretical model is presented to describe the charge carrier transport mechanism and to quantitatively estimate the barrier heights. These results can benefit recent topical approaches for graphene integration in various semiconductor devices. © *2012 American Institute of Physics*. [http://dx.doi.org/10.1063/1.3696671]

Graphene-semiconductor contact is of critical importance to the fabrication of high-performance graphene electronic and optoelectronic devices.[1–8] Approaches have been reported for graphene integration in semiconductor devices, including GaN and organic light-emitting diodes (LED)[4–6] and silicon and polymer-based photovoltaic cells.[8–10] In these applications, the electronic contact properties of the interfaces between graphene and the semiconductor play a key role in device performance, such as the turn-on voltage of LEDs (Ref. 4) and the photoelectrical efficiency of solar cells.[8] Therefore, the carrier transport and the interactions between semiconductor substrates and graphene sheets have attracted increasing attention recently.[11–14] Barrier heights have been measured between few-layer or a mix of single-layer, bi-layer, and few-layer graphene and a semiconductor.[2,3,8] The junctions between them have been described as traditional Schottky diodes with an invariant Fermi level of graphene-like metal. However, the Fermi level in graphene can be shifted by the charge carrier transport,[15,16] which subsequently affects barrier heights. For neutral single-layer graphene (SLG), the Fermi level is aligned with Dirac points and the density of states (DOS) vanishes exactly at this point.[17] It can be calculated that a transfer of 0.01 electrons per unit cell would shift the Fermi level by 0.47 eV.[18] This behavior is quite different from that of conventional metals, in which the charge transport can barely vary the Fermi level because of their high DOS at the Fermi energy. Systematic experimental studies and theoretical modeling of the graphene-semiconductor junctions are clearly needed.

As we know, the Fermi level difference and the associated charge transport are the main contributors to the high-resistance Schottky barrier in the contact between conventional metals and semiconductors.[19] By applying the distinct electronic property of graphene mentioned above, we claim that graphene has a potential ability to form low barrier height contacts to both *n*- and *p*-type semiconductors. When graphene is in contact with *n*-type semiconductor [Figs. 1(a) and 1(b)], the electron transport from the bulk *n*-type semiconductor into the graphene will raise up the graphene's Fermi level from the Dirac points towards that of the *n*-type semiconductor and the barrier heights will be reduced. Similarly, the holes transport from the *p*-type semiconductor to graphene will also result in a reduction of the barrier height.

In this study, SLG sheets were prepared by micromechanical exfoliation of Kish graphite[20] on both native *n*-type gallium nitride (*n*-GaN) and Mg-doped *p*-type gallium nitride (*p*-GaN) substrates for comparative studies. The number of graphene layers was identified using spectroscopy (JY LabRam HR 800) with a 632.8 nm wavelength laser. Both *n*-GaN and *p*-GaN films were grown on (0001) sapphire by the metal-organic chemical vapor deposition (MOCVD) method. Their carrier density characterized by Hall measurements were $5.0 \times 10^{18}\,\mathrm{cm}^{-3}$ and $4.5 \times 10^{17}\,\mathrm{cm}^{-3}$, respectively. The topography of the samples was characterized by atomic force microscopy (AFM) (NT-MDT NTEGRA Spectra) in tapping mode. The contact properties of graphene-GaN were studied using conductive atomic force microscopy (C-AFM) in contact mode with an Au-coated tip. Meanwhile, bias voltages

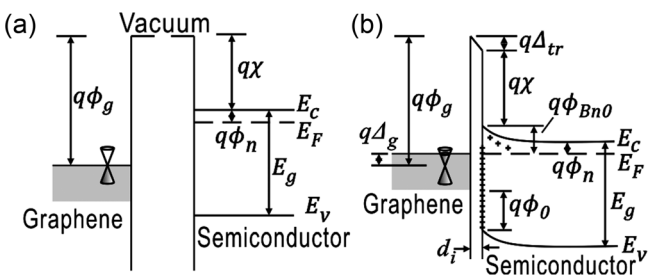

FIG. 1. (a) Graphene and *n*-type semiconductor in separated systems. (b) Graphene and *n*-type semiconductor connected into one system in which the effect of interfacial states is also taken into account. Definition of symbols: ϕ_m and ϕ_g are the work functions of metal and neutral graphene, respectively. χ is the electron affinity of the semiconductor and E_g is band gap. $q\phi_n$ is the energy difference between the bottom energy of the conduction band E_c and the Fermi level E_F. ϕ_{Bn0} is the barrier height. ϕ_0 is the neutral level of the interfacial states above valance band E_v. Δ_g is the work function shift of graphene relative to the Dirac points. Δ_{tr} is the potential drop on the interfacial gap *di* between graphene.

[a)]Haijian Zhong and Zhenghui Liu contributed equally to this work.
[b)]Electronic mail: kxu2006@sinano.ac.cn.
[c)]Electronic mail: hyang2006@sinano.ac.cn.

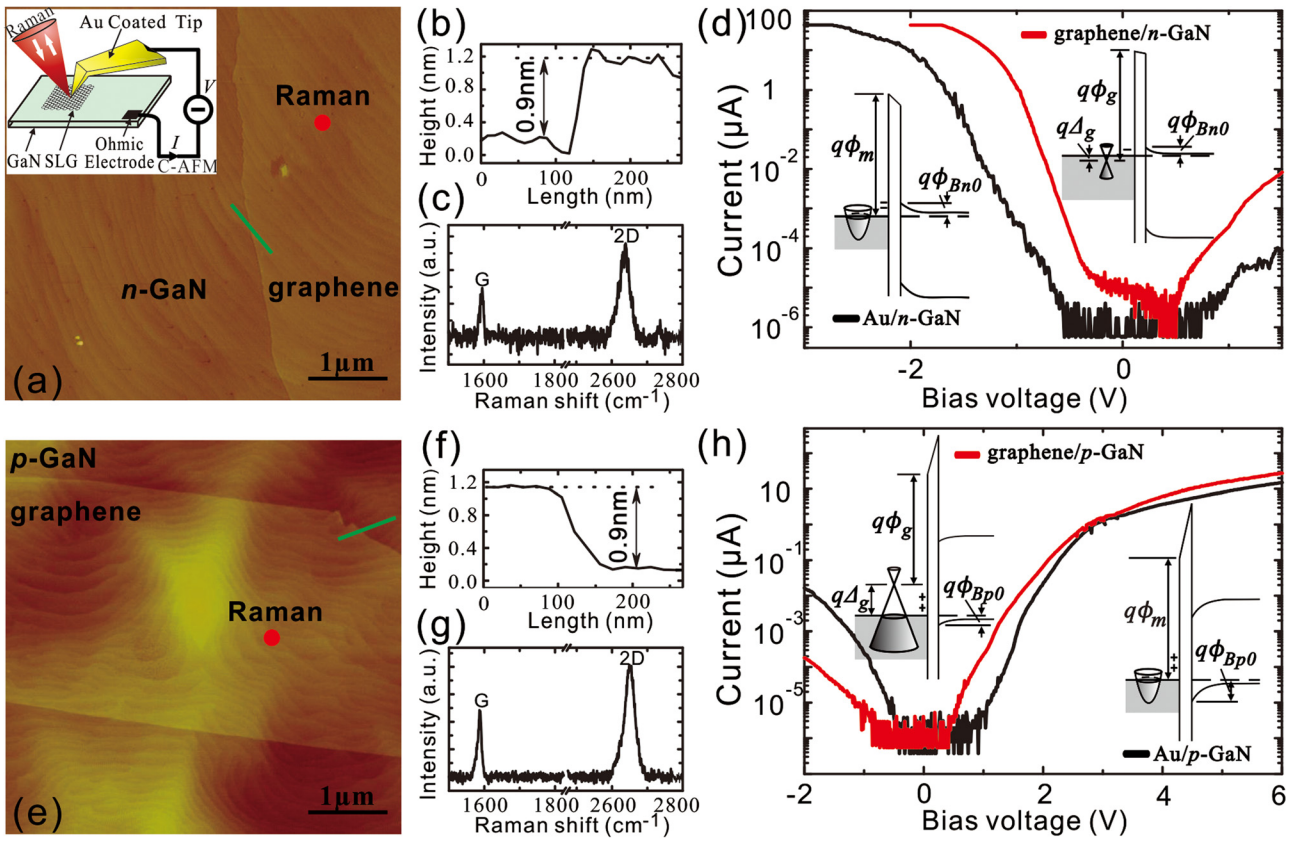

FIG. 2. Tapping mode AFM images of an isolated SLG sheet on an *n*-GaN (a) and a *p*-GaN (e) substrate. The green lines across the boundary between graphene and GaN indicate the profile for the heights shown in (b) and (f) at approximately 0.9 nm for both the *n*-GaN and *p*-GaN samples. Inset: Diagram of integrated C-AFM and Raman measurements with an Au-coated AFM tip. (c) and (g) Raman spectra (632.8 nm laser wavelength) obtained from the corresponding red spots in (a) and (e). a.u., arbitrary units. (d) and (h) Local *I-V* curves, acquired from bare *n*- and *p*-GaN (black lines) substrates and graphene sheets (red lines), respectively. Insets: schematic band structures of Au/*n*-GaN and graphene/*n*-GaN in (d) and Au/*p*-GaN and graphene/*p*-GaN in (h), which demonstrates the barrier heights and the Fermi level shift. The values are listed in Table I.

were applied to GaN substrates through conventional metal ohmic electrodes [Fig. 2(a), inset].

Figures 2(a) and 2(e) show the topography of an isolated SLG sheet on an *n*-GaN and a *p*-GaN substrate, respectively. Unlike previous studies of mechanically cleaved SLG on smooth substrates, such as SiO_2 or mica, the transferred SLG sheets on the growth face of GaN have spread along the GaN terraces. To eliminate the effects of corrugations from GaN terraces, AFM line profiles should be on the same GaN terrace and should cross the boundary between graphene and GaN. The step heights of the graphene sheets [Figures 2(b) and 2(f)] have been determined to be 0.9 ± 0.2 nm both for the *n*-GaN and *p*-GaN samples. These values are approximate to the reported height values of about 1.0 nm on other substrates.[16] Raman spectra [Figs. 2(c) and 2(g)] confirmed that the graphene sheets consist of a single layer.

Typical current-voltage (*I-V*) curves are plotted for *n*- and *p*-GaN in Figures 2(d) and 2(h), respectively, in which the black curves were acquired on bare GaN surfaces and the red ones were acquired on graphene covered area. An obvious rectifying behavior similar to a Schottky barrier is observed. The barrier height ϕ_{Bn0} can be obtained by the least squares method using the expression[19] $I = AA^*T^2\exp(-q\phi_{Bn0}/(kT))[\exp(qV/(\eta kT)) - 1]$, where A is the contact area, A^* is the Richardson constant (26.4 A cm^{-2} K^{-2} for *n*-GaN and 96.1 A cm^{-2} K^{-2} for *p*-GaN), and η is the ideality factor. Taking ϕ_{Bn0}, A and η as fitting parameters, the barrier heights between the Au tip and *n*-GaN were 0.50 ± 0.05 V determined statistically as shown in Table I. When the Au tip was moved onto the SLG, the fitted barrier heights were reduced to 0.33 ± 0.01 V. Similar results were obtained from *p*-GaN. The statistical barrier height was -0.87 ± 0.23 V on bare *p*-GaN and was reduced to -0.36 ± 0.02 V on the graphene-covered surface. Noting the large band gap width of 3.4 eV of GaN, the above experimental results verified our assumption that graphene can adapt its Fermi level to either type of GaN when they are in contact and result in lower barrier heights. The schematic band structures after contact are shown in the insets of Figures 2(d) and 2(h).

To quantitatively estimate the barrier heights and Fermi level shift of graphene, we presented a model and considered the case of *n*-GaN. There are three key differences between this model and traditional Schottky barrier theory. First, the

TABLE I. The calculated and experimental barrier heights (symbols are marked in the insets of Figures 2(d) and 2(h)).

	Calculations			Experiments
Junctions	ϕ_m/ϕ_g (V)	Δ_g (V)	ϕ_{Bn0}/ϕ_{Bp0} (V)	ϕ_{Bn0}/ϕ_{Bp0} (V)
Au/n-GaN	5.1	—	—	0.50 ± 0.05
SLG/n-GaN	4.6	0.15	0.32	0.33 ± 0.01
Au/p-GaN	5.1	—	—	-0.87 ± 0.23
SLG/p-GaN	4.6	−1.27	−0.39	-0.36 ± 0.01

metal tip will easily form ohmic contact with graphene.[21] In accordance with the very high in-plane mobility of carriers with the theoretical Fermi velocity $v_F = 1 \times 10^6$ m/s in graphene,[17] the current from the tip will immediately diffuse in graphene films and then transmit to GaN. The electronic properties are dominated by the interfaces between graphene and GaN. The influence of the metal tip with an apex of about 10-30 nm can be neglected here. This approximation can be justified from our measurements using AFM tips with different metal coatings. The barrier heights between graphene and GaN measured by the Pt-coated tip (0.40 ± 0.04 V for graphene/*n*-GaN and 0.37 ± 0.03 V for graphene/*p*-GaN) are very close to those measured by the Au tip. Second, different from conventional metal, the work function of SLG is floating when it is negatively or positively charged because graphene is a monolayer with low density of states. The linear DOS of graphene in the vicinity of the Dirac points is:[17] $\rho(E) = [2\pi^{-1}(\hbar v_F)^{-2}]|E| = D_0|E|$, where E is the energy with $E = 0$ eV at the Dirac points. By integrating the linear DOS, we obtain a relationship between the charge Q_G transferred into the graphene and the resulting Fermi level shift Δ_g

$$\Delta_g = -\mathrm{sign}(Q_G)\sqrt{2|Q_G|/(q^3 D_0)}, \tag{1}$$

where q is the elementary charge. Third, similar to a metal-graphene contact,[18] there exists an interface separation d_i of a few angstroms between graphene and GaN, which is transparent for carriers but creates an additional potential drop Δ_{tr}. The value can be obtained by applying Gauss' law to the surface charge on the graphene and GaN

$$\Delta_{tr} = -Q_G \cdot d_i/(\varepsilon_i \varepsilon_0), \tag{2}$$

where ϵ_i is the relative dielectric constant for the region between graphene and GaN. The value is taken as 10.4 equaling to that of GaN. The value of d_i can be estimated as 0.6 nm by subtracting the thickness of SLG (0.34 nm) from the experimental step height of the graphene measured by AFM (0.9 nm).

Applying the "box profile" approximation in semiconductors, the space charge density in the depletion region of *n*-GaN is[19]

$$Q_s = \mathrm{sign}(\phi_{Bn0} - \phi_n - kT/q)\sqrt{2q\varepsilon_r\varepsilon_0 n|\phi_{Bn0} - \phi_n - kT/q|}, \tag{3}$$

where ϕ_{Bn0} is the barrier height, $\epsilon_r = 10.4$ is the relative dielectric constant of GaN, n is the carrier density, and ϕ_n is the energy difference between the bottom energy of conduction band E_c and the Fermi level E_g. Since the experimental barrier height of the Au/*n*-GaN (0.50 ± 0.05 V) is lower than their Fermi level difference (1.0 V), the interface charge density Q_i induced by the interfacial states of *n*-GaN cannot be ignored. Here, we describe the interfacial states by the neutral level ϕ_0 and DOS D_{it}, as with conventional metal-semiconductor theory.[19] ϕ_0 is the energy level above E_V at a semiconductor surface, which is negatively charged when $E_F > q\phi_0$ and positively charged when $E_F < q\phi_0$. Assuming that the DOS of interfacial states is D_{it} states/(cm^2 eV), the interface charge density on *n*-GaN can be calculated using

$$Q_i = -qD_{it} \cdot (E_g - q\phi_0 - q\phi_{Bn0}). \tag{4}$$

If ϕ_0 and D_{it} are properties of the GaN surface and are independent of the contact material, their values can be calculated from the barrier heights measured on a bare GaN surface by the Au- and Pt-coated tips, respectively.[19] For our *n*-GaN sample, the measured barrier-heights for Au- and Pt-coated tips are 0.50 ± 0.05 V and 0.65 ± 0.03 V, respectively. The calculated values of ϕ_0 and D_{it} are 3.10 V and 3.02×10^{14} ev^{-1}cm^{-2}, respectively. For our *p*-GaN sample, the measured barrier-heights for Au- and Pt-coated tips are -0.87 ± 0.23 V and -0.60 ± 0.05 V, respectively. The calculated values of ϕ_0 and D_{it} are -0.61 V and 1.18×10^{14} ev^{-1}cm^{-2}, respectively.

The balance of charge in the graphene, the interface, and the depletion region of GaN gives $Q_G = -(Q_i + Q_s)$, where the Q_i and Q_s can be substituted by Eqs. (3) and (4). By substituting the Q_G in Eqs. (1) and (2), both Δ_{tr} and Δ_g can be expressed as the function of ϕ_{Bn0}. As illustrated in Figure 1(b), the alignment of the Fermi level between the graphene and GaN gives the equation: $\phi_g - \chi = \Delta_g + \Delta_{tr} + \phi_{Bn0}$, where ϕ_g is the work function of neutral graphene (4.6 V) and χ is the affinity of GaN (4.1 V). Then, the ϕ_{Bn0} can be solved numerically.

The calculated barrier heights with this model are displayed in Table I. They are in accordance with those fitted from the measured *I-V* curves with CAFM. The calculated Fermi level shifts of graphene are also listed in Table I. It should be noted that the Fermi level shift of graphene depends on the amount of transferred charge both from the interfacial states (Q_i) and from the depletion region of semiconductor (Q_s). The calculated Q_i and Q_s are -3.4×10^{-7} C/cm^2 and 6.8×10^{-7} C/cm^2, respectively, for graphene/*n*-GaN and are -1.9×10^{-5} C/cm^2 and -2.2×10^{-7} C/cm^2, respectively for graphene/*p*-GaN. The transferred charge from the interfacial states of graphene/*p*-GaN is approximately two orders of magnitude higher than that of graphene/*n*-GaN. This is attributed to the larger difference between the neutral level ϕ_0 of interfacial states and the Dirac point of graphene. Therefore, the graphene on *p*-GaN is more heavily doped and the Fermi level shift is much larger than the one in the *n*-GaN case.

As a compare, assuming the Fermi level of graphene were kept unchanged with $\phi_g = 4.6$ V before and after contacting with GaN, the barrier heights of graphene/*n*-GaN and graphene/*p*-GaN can be calculated out to be 0.36 V and -0.95 V, which deviate from the experimental results.

In conclusion, due to the low and linear density of states, SLG can shift its Fermi level by charging and then adapt towards the semiconductor's Fermi level. This unique property in graphene has been demonstrated in our experimental results to lower the barrier height between graphene and a semiconductor of both *n*-GaN and *p*-GaN. A theoretical model was presented to elaborate the mechanism of self-adaptive electronic contact between graphene and semiconductors and quantitatively estimate the barrier heights. These approaches provide deep insight into the physics of graphene-semiconductor contacts, which will also benefit recent topical research to incorporate graphene into various semiconductor devices.

We thank H. B. Wang for assistance in fabrication. This work was supported by the Instrument Developing Project, CAS (YZ200939), the NSF (10904107, 10974141, 10704052, 776003, and 10804081), and the NBRP (973 program) of China (2007CB936701).

[1]F. Bonaccorso, Z. Sun, T. Hasan, and A. C. Ferrari, Nature Photon. **4**, 611 (2010).
[2]C. Chen, M. Aykol, C. Chang, A. F. J. Levi, and S. B. Cronin, Nano Lett. **11**, 1863 (2011).
[3]S. Tongay, T. Schumann, X. Miao, B. R. Appleton, and A. F. Hebard, Carbon **49**, 2033 (2011).
[4]K. Chung, C. H. Lee, and G. C. Yi, Science **330**, 655 (2010).
[5]G. Jo, M. Choe, C. Y. Cho, J. H. Kim, W. Park, S. Lee, W. K. Hong, T. W. Kim, S. J. Park, and B. H. Hong, Nanotechnology **21**, 175201 (2010).
[6]T. Sun, Z. L. Wang, Z. J. Shi, G. Z. Ran, W. J. Xu, Z. Y. Wang, Y. Z. Li, L. Dai, and G. G. Qin, Appl. Phys. Lett. **96**, 133301 (2010).
[7]S. Tongay, T. Schumann, and A. F. Hebard, Appl. Phys. Lett. **95**, 222103 (2009).
[8]X. M. Li, H. W. Zhu, K. L. Wang, A. Y. Cao, J. Q. Wei, C. Y. Li, Y. Jia, Z. Li, X. Li, and D. H. Wu, Adv. Mater. **22**, 2743 (2010).
[9]K. Ihm, J. T. Lim, K. Lee, J. W. Kwon, T. Kang, S. Chung, S. Bae, J. H. Kim, B. H. Hong, and G. Y. Yeom, Appl. Phys. Lett. **97**, 032113 (2010).
[10]Y. Gao, H. Yip, S. K. Hau, K. M. O'Malley, N. C. Cho, H. Chen, and A. K. Y. Jen, Appl. Phys. Lett. **97**, 203306 (2010).
[11]K. T. He, J. C. Koepke, S. Barraza-Lopez, and J. W. Lyding, Nano Lett. **10**, 3446 (2010).
[12]L. Magaud, F. Hiebel, F. Varchon, P. Mallet, and J. Y. Veuillen, Phys. Rev. B **79**, 161405 (2009).
[13]A. Mattausch and O. Pankratov, Phys. Rev. Lett. **99**, 76802 (2007).
[14]S. Y. Zhou, G. H. Gweon, A. V. Fedorov, P. N. First, W. A. De Heer, D. H. Lee, F. Guinea, A. Neto, and A. Lanzara, Nature Mater. **6**, 770 (2007).
[15]Z. Y. Chen, I. Santoso, R. Wang, L. F. Xie, H. Y. Mao, H. Huang, Y. Z. Wang, X. Y. Gao, Z. K. Chen, and D. G. Ma, Appl. Phys. Lett. **96**, 213104 (2010).
[16]K. S. Novoselov, A. K. Geim, S. V. Morozov, D. Jiang, Y. Zhang, S. V. Dubonos, I. V. Grigorieva, and A. A. Firsov, Science **306**, 666 (2004).
[17]A. H. Castro Neto, F. Guinea, N. Peres, K. S. Novoselov, and A. K. Geim, Rev. Mod. Phys. **81**, 109 (2009).
[18]G. Giovannetti, P. A. Khomyakov, G. Brocks, V. M. Karpan, J. van den Brink, and P. J. Kelly, Phys. Rev. Lett. **101**, 26803 (2008).
[19]S. M. Sze and K. K. Ng, *in Physics of Semiconductor Devices*, 3rd ed. (Wiley, Hoboken, 2007).
[20]K. S. Novoselov, D. Jiang, F. Schedin, T. J. Booth, V. V. Khotkevich, S. V. Morozov, and A. K. Geim, Proc. Natl. Acad. Sci. U.S.A. **102**, 10451 (2005).
[21]K. Nagashio, T. Nishimura, K. Kita, and A. Toriumi, Appl. Phys. Lett. **97**, 143514 (2010).